Preparation of Gd-doped EuO_{1-x} thin films and the magnetic and magneto-transport properties

2004 J. Phys.: Condens. Matter 16 6017

(http://iopscience.iop.org/0953-8984/16/34/003)

INSTITUTE OF PHYSICS PUBLISHING JOURNAL OF PHYSICS: CONDENSED MATTER

J. Phys.: Condens. Matter **16** (2004) 6017–6028 PII: S0953-8984(04)74538-5

Preparation of Gd-doped EuO_{1-x} thin films and the magnetic and magneto-transport properties

Tetsuro Matsumoto[1,2], Katsuhiko Yamaguchi[3], Masatada Yuri[4], Kenji Kawaguchi[2], Naoto Koshizaki[2] and Koji Yamada[1]

[1] Department of Material Sciences, Saitama University, 255 Shimo-ohkubo, Saitama City, Saitama 338-8570, Japan
[2] National Institute of Advanced Industrial Science and Technology (AIST), Central 5, 1-1-1 Higashi, Tsukuba, Ibaraki 305-8565, Japan
[3] Faculty of Education, Fukushima University, 1 Kanayagawa, Fukushima 960-1296, Japan
[4] National Synchrotron Radiation Research Center, Hsinchu Science-Based Industrial Park, Hsinchu 30077, Taiwan

Received 9 January 2004
Published 13 August 2004
Online at stacks.iop.org/JPhysCM/16/6017
doi:10.1088/0953-8984/16/34/003

Abstract

Polycrystalline europium monoxide (EuO) films doped with and without Gd were prepared using a reactive deposition method in a MBE system. Two different electron doping methods, Gd substitution and oxygen deficiency, enhance the Curie temperature (T_C) and the temperature dependence of magnetization differently. Gd doping increases T_C up to 125 K, while oxygen deficient samples enhance it above 150 K. The enhanced T_C is attributed to the increase in the indirect exchange interaction between Eu^{2+} spins via conduction electrons. The resistivities as a function of temperature for both quasi-stoichiometric (QS) EuO and QS-$Gd_xEu_{1-x}O$ show maxima near 70 and 110 K, respectively. The conduction band magnetic splitting explains the resistivity behaviours. Both the temperature dependences of the large magneto-resistance and the absorption edge are also interpreted by the conduction band magnetic splitting mechanism. The unusual blue shift observed in Gd-doped samples is not yet understood.

1. Introduction

Recently, the term 'spintronics', which means adding a spin degree of freedom to conventional charge-based electronics, has become popular as a next generation device concept that will open a new world of highly functional electronic devices. High density, high speed, nonvolatile, and energy efficient new devices are expected from spintronics [1]. In fact, MRAM (magnetic

random access memory), a spintronics device, is currently being developed. Thus, carrier-induced magnetization is an attractive phenomenon not only in basic physics, but is a key technology in spintronics as a charge–spin converter. Recently, carrier-induced magnetization in III–V magnetic semiconductors doped with 3d magnetic elements such as (In, Mn)As have been actively studied [2]. In these cases, the Mn doping introduces holes to the valence band, which induce a long range ferromagnetic ordering of the local magnetic moments at 3d-element sites via a p–d type exchange interaction [3, 4]. This means that carrier doping or other external factors can change the intrinsic material properties. Actually, the electrical manipulation of magnetism is realized in an (In, Mn)As field-effect transistor structure. Applying negative gate bias enhances the ferromagnetic interaction between Mn ions as the hole concentration increases and ultimately (In, Mn)As becomes a ferromagnet [5]. On the other hand, the transport and optical properties of europium chalcogenides (EuX, X = O, S, Se, Te) have been studied as typical magnetic semiconductors [6]. In particular, EuO and EuS receive a lot of attention as valuable n-type ferromagnetic semiconductors. The characteristic correlation between conduction electrons and magnetization as described later suggests a promising spintronics material. Another possible spintronics application for a spin injector is the idea of a spin filter with a tunnel junction structure [7]. Numerous experimental results have been reported for bulk pure and doped EuO [8]. Although EuO films are important in device applications, they are not actively studied, which may be due to the difficulty in preparing stable EuO thin films [9–14]. Film samples are also very effective for basic material research including transmission spectroscopy, transport measurements, uniform doping, and structural modification. Thus, we tried to prepare high quality films with and without Gd doping to investigate the physical properties.

Several basic physical properties of pure and doped EuO have been studied using bulk samples. The temperature dependence of magnetization (M–T curve) for stoichiometric EuO satisfies Brillouin's law with a spin 7/2, and the ferromagnetic transition is observed around 70 K. The molecular field approximation (MFA) explains the magnetic property of stoichiometric EuO [8]. Since the electron concentration of the conduction 5d band can be controlled by doping with certain trivalent ions, Gd-doped europium oxide $Gd_xEu_{1-x}O$ has been extensively studied to clarify the relationship between carrier concentration and Curie temperature (T_C). The enhanced T_C above 70 K on Gd doping implies a strong dependence of the magnetic interaction on the carrier electron concentration [8, 15]. Uniform doping and negligible structural changes are expected since gadolinium is next to europium in the periodic table. The same half-filled $4f^7$ electronic configurations of Eu^{2+} and Gd^{3+} are also favourable for a doping study. The oxygen vacancy (EuO_{1-x}) also provides electrons to the conduction band and enhances T_C to approximately 150 K [14, 16]. The measured M–T curves of both n-type samples significantly deviate from Brillouin's law above T_C of stoichiometric EuO. Two exchange interactions J_1 and J_2 are considered for the EuO ferromagnetic ordering, which are the nearest neighbour and next nearest neighbour Eu^{2+}–Eu^{2+} interactions, respectively [8]. Some enhancement mechanism in J_1 and J_2 or another novel magnetic interaction is necessary to explain this higher T_C by carrier doping. For the enhanced $J_{1,2}$, the magnetization behaviour should follow Brillouin's law with a higher T_C since the substantial magnetic mechanism does not change. However, the measured M–T curves of n-type EuO clearly do not follow Brillouin's law. Thus, the idea that doped electrons enhance T_C via 4f–5d indirect exchange interactions (J_{df}) between 4f Eu^{2+} local and 5d conduction electron spins is proposed [8]. The total exchange interaction may increase with the 5d electron doping. Therefore, an EuO doping study should elucidate this interaction mechanism. This paper reports the preparation and the magnetic, transport, and optical properties of electron doped EuO thin films, i.e. $Gd_xEu_{1-x}O$ and EuO_{1-x}.

2. Sample preparation

Sample films were prepared by a reactive deposition method in an ultra-high vacuum deposition apparatus. The growth chamber was initially evacuated to $\sim 1.0 \times 10^{-9}$ Torr and then oxygen was introduced as described below. The outgas from the Eu source increased the base pressure to a range near 10^{-7} Torr during Eu evaporation by a Knudsen cell. Hydrogen is the dominant atomic species of the outgas. Since Eu is easily oxidized to Eu_2O_3, the oxygen pressure must be precisely controlled in the range of 10^{-7} Torr for high quality EuO, but the background hydrogen relative to the necessary oxygen pressure makes precise pressure control difficult. Consequently, a quadrupole mass spectrometer (QMAS) was employed to monitor the oxygen partial pressure. Oxygen gas was initially introduced with the pressure of the deposition condition before heating the Eu source and the oxygen inlet valve was adjusted to maintain a constant mass number 32 (O_2) signal intensity by QMAS monitoring during deposition. The deposition rate, another important condition, was maintained at 2.0 Å s^{-1} using an *in situ* oscillation crystal thickness monitor. The substrates were quartz glass plates. The substrate temperature was fixed at 300 °C and the sample thickness ranged from 200 to 2000 Å. An aluminium or calcium fluoride capping layer was finally deposited to protect the sample films. To prevent a reaction between Eu and capping layer, the substrate was not heated. Especially when CaF_2 was the capping layer, EuO was easily converted to $Eu(OH)_3$. To prevent the hydroxylation, the sample films were pretreated with Ar gas in the introduction chamber. The pretreatment effects were unclear, but hydroxylation of EuO was suppressed [18]. For x-ray diffraction (XRD) and magnetic measurements, aluminium was used as a capping layer due to the chemical stability, low x-ray absorption, and good coverage. Since an Al capping layer causes an electric short circuit and is not transparent to visible and near-infrared light, CaF_2 was employed to measure the electric transport and optical properties. Both XRD and magnetization measurements were indifferent to Al and CaF_2 capping. The thickness of capping layer was 2500 Å for most samples. The samples removed from the MBE chamber were handled in a glove box filled with Ar gas. The variations of T_C as a function of Gd concentration were calculated for $Gd_xEu_{1-x}O$ [17]. The calculated maximum T_C was above 150 K at $x = 0.05$. Thus, Gd doping in the range of 0.5–5.0 atomic per cent was examined. The doped samples were prepared by the same reactive deposition method as EuO thin films except for the co-evaporation of Gd and Eu metal sources.

3. Sample structure

An usual powder XRD method was used to investigate the structural properties of our samples. As shown in figure 1, EuO stacking planes are almost aligned with ⟨200⟩ orientation. In spite of the preferred orientation patterns, the broad rocking curves indicate that the sample films are not epitaxially grown. Since the structural properties of europium oxide are very sensitive to the preparation conditions, some samples display EuO⟨111⟩ or metal Eu peaks due to the small change in the conditions. Table 1 lists the peak positions and full widths at half maximum (FWHMs) obtained by Gaussian curve fitting for four typical samples in figure 1. The measured XRD peak positions include instrumental offsets; therefore, the relative difference between ⟨200⟩ and ⟨111⟩ diffraction angles is more reliable. All calculated differences are within $4.82° \pm 0.03°$ in 2θ, which implies negligible lattice distortion from oxygen deficiency and Gd doping. Small FWHMs, less than 0.4°, indicate relatively good crystallinity. The doped Gd concentration is examined by a scanning electron microscope (SEM) equipped with an energy dispersive x-ray spectrometer (EDX). The measured results are within the designed values ±1%, which is a small deviation considering the EDX experimental error.

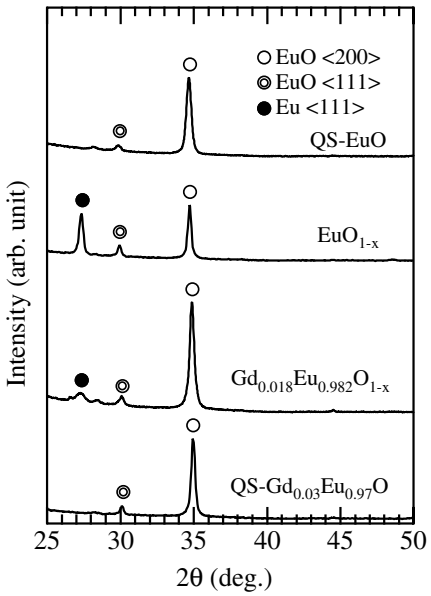

Figure 1. XRD spectra for QS-EuO, EuO_{1-x}, $Gd_{0.018}Eu_{0.982}O_{1-x}$, and QS-$Gd_{0.03}Eu_{0.97}O$ measured by Cu Kα radiation.

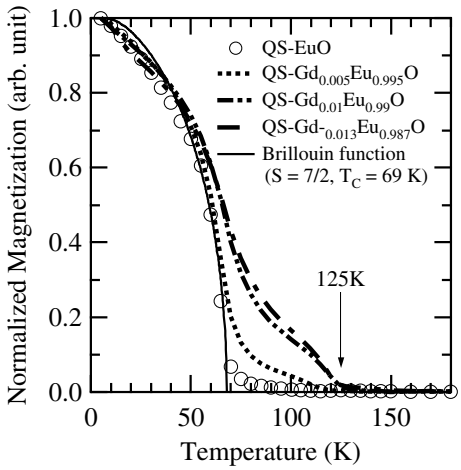

Figure 2. Magnetization curves as a function of temperature for QS-EuO and $Gd_xEu_{1-x}O$ ($x = 0.005$, 0.01, 0.013) films and Brillouin function for $S = 7/2$, $T_C = 69$ K (solid curve). The magnetization measurements were performed with a 10 mT field in the sample plane. The plotted data are normalized at 5 K.

Table 1. Peak position and full width at half maximum of fitted XRD patterns.

	EuO		EuO_{1-x}		$Gd_{0.018}Eu_{0.982}O_{1-x}$		$Gd_{0.03}EuO_{0.97}$	
	⟨200⟩	⟨111⟩	⟨200⟩	⟨111⟩	⟨200⟩	⟨111⟩	⟨200⟩	⟨111⟩
Peak position (deg)	34.67	29.84	34.72	29.93	34.88	30.06	34.95	30.10
Difference between ⟨200⟩ and ⟨111⟩ (deg)	4.83		4.79		4.82		4.85	
FWHM (deg)	0.352	0.369	0.258	0.242	0.344	0.320	0.283	0.243

4. Magnetic properties

The temperature dependence of the magnetization was measured using a superconducting quantum interference device (SQUID) magnetometer. Figure 2 shows the results for quasi-stoichiometric EuO and $Gd_xEu_{1-x}O$ ($x = 0.005, 0.01, 0.013$) samples. Since the paramagnetic susceptibility for the samples is relatively large near T_C, the temperature dependence is measured with a small applied field (10 mT) instead of a saturation field. All the magnetization curves are normalized to unity at $T = 5$ K to clarify the difference of temperature dependence of the magnetization. These QS-EuO and QS-$Gd_xEu_{1-x}O$ give saturated magnetizations (M_Ss) between 5.8 and 6.3 μ_B/atom at 5 K, which are 83–90% of the ideal full moment (7 μ_B) as shown in table 2. In this report, EuO with a T_C around 70 K is defined as quasi-stoichiometric EuO (QS-EuO). Gadolinium-doped samples prepared under the same conditions as QS-EuO are defined as quasi-stoichiometric $Gd_xEu_{1-x}O$ (QS-$Gd_xEu_{1-x}O$). The magnetization curve of QS-EuO is well fitted to the Brillouin function ($S = 7/2$) with a T_C of 69 K. The magnetic

Table 2. The saturated magnetization of QS-EuO and QS-$Gd_xEu_{1-x}O$ plotted in figure 2 measured by SQUID magnetometer. The magnetic field is applied up to 7 T in the sample plane.

Sample	M_S (μ_B/atom)
QS-EuO	6.3
QS-$Gd_{0.005}Eu_{0.995}O$	5.8
QS-$Gd_{0.01}Eu_{0.99}O$	6.1
QS-$Gd_{0.013}Eu_{0.987}O$	6.0

behaviour is the same simple Heisenberg ferromagnet as bulk EuO [8]. However, the curves of QS-$Gd_xEu_{1-x}O$ ($x = 0.005$, 0.01, 0.013) significantly deviate from Brillouin's law above 70 K and enhance T_C up to 120–125 K. The lack of a metal Gd peak in the XRD spectrum of $Gd_xEu_{1-x}O$ indicates that Gd successfully substituted for Eu atoms. Both the Gd^{3+} ion absorption spectrum and the same T_C for Eu^{2+} and Gd^{3+} sites observed in x-ray absorption spectroscopy (XAS) and x-ray magnetic circular dichroism (XMCD) measurements [19] provide evidence that Gd uniformly and ideally substitutes for Eu. Accordingly, the enhanced T_C in $Gd_xEu_{1-x}O$ is attributed to Gd doping. In bulk $Gd_xEu_{1-x}O$ samples, the enhanced T_C is understood by the indirect exchange interaction (J_{df}) mediated via doped carrier electrons in the conduction band. Mauger *et al* reported that the enhancement is dependent on the carrier electron concentration [8]. For a lower Gd concentration, since the charge carriers are localized around the Gd donors, electrons are not introduced into the conduction band. Thus, T_C is unchanged for x less than critical concentration (N_C). The estimated critical carrier concentration is $\sim 10^{20}$ cm^{-3} at room temperature for bulk $Gd_xEu_{1-x}O$ [8]. Since each Gd ion provides one electron to the conduction band, the estimated N_C can be converted to the critical Gd concentration X_C ($\sim$1.2 at.%). In bulk stoichiometric EuO samples, the carrier electron concentration N is $\sim 10^{18}$ cm^{-3} less than N_C [8] and the magnetization curve follows Brillouin's law with $T_C \sim 70 \pm 1$ K. A remarkable increase in T_C should be observed at $N \sim N_C$ according to the simple Mauger mechanism. In spite of doping levels less than X_C ($\sim$1.2 at.%), the T_C of QS-$Gd_{0.005}Eu_{0.995}O$ is enhanced up to 120 K (figure 2). The magnetization of QS-$Gd_xEu_{1-x}O$ clearly increases from $x = 0.005$ to 0.01 and slightly above 0.01 in the temperature range from 80 to 120 K. The enhanced T_C and increased magnetization suggest N_C is less than 0.5 at.% since the d–f magnetic interaction is abruptly enhanced just above N_C by Mauger's mechanism [8].

Figure 3 also shows the deviation in the magnetization of non-stoichiometric samples from Brillouin's law. A characteristic dent is observed from 10 to 20 K for both non-stoichiometric $Gd_{0.02}Eu_{0.98}O_{1-x}$ and undoped EuO_{1-x} samples. This dent is found in other oxygen deficient samples and may be due to the magnetization of the residual metal Eu clusters. A metal Eu film was prepared without oxygen gas to confirm the dent. The magnetization of the Eu metal significantly increases below 20 K as shown in figure 3. To make the dent negligible during the manual process, the weighted Eu magnetization was subtracted from $Gd_{0.02}Eu_{0.98}O_{1-x}$ and EuO_{1-x} magnetization. Smooth, Brillouin-like magnetization curves were successfully obtained as plotted in figure 4. The evaluated residual metal Eu from the subtraction was about 12 at.% for both $Gd_{0.02}Eu_{0.98}O_{1-x}$ and EuO_{1-x}, which suggests a good reproducibility of our samples.

As shown in figure 4, a higher T_C of 160 K is observed for EuO_{1-x} compared to 125 K for QS-$Gd_xEu_{1-x}O$ samples. The magnetization curve of $Gd_{0.02}Eu_{0.98}O_{1-x}$ exhibits a significant drop around 125 K and finally reaches zero at 160 K. The magnetization profile overlaps the Gd-doped and oxygen deficient EuO. The same n-type dopings by Gd and oxygen vacancy seem to enhance the temperature dependence of the magnetic interaction differently. Gadolinium

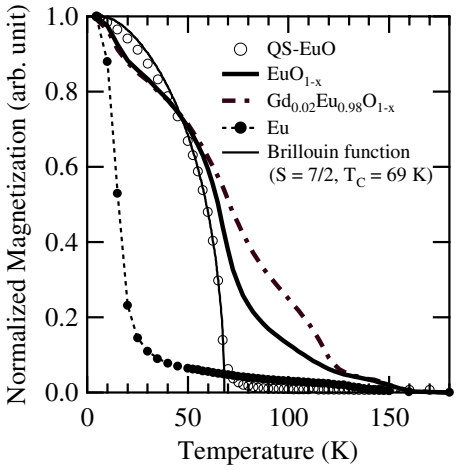

Figure 3. Magnetization curves as a function of temperature for QS-EuO, EuO_{1-x}, $Gd_{0.02}Eu_{0.98}O_{1-x}$, and metal Eu. The magnetization measurements were performed with a 10 mT field in the sample plane. The plotted data are normalized at 5 K.

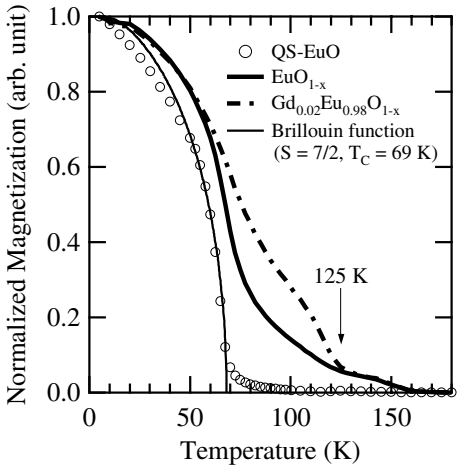

Figure 4. The magnetization curve of EuO_{1-x} in figure 3 corrected using the Eu result. The oxygen deficiencies of EuO_{1-x} and $Gd_{0.02}Eu_{0.98}O_{1-x}$ are equivalent.

doping provides one carrier electron per Gd atom to the impurity level or conduction band, while a vacant oxygen provides two electrons. The depth and extent of the donor level might be different for each case. However, the details of the impurity levels are unclear [21].

Figure 5 plots the magnetization difference (ΔM), which clarifies the co-existence of two different contributions from Gd doping and oxygen vacancies. The difference between QS-$Gd_{0.01}Eu_{0.99}O$ and QS-EuO (thick solid curve) implies that there is a Gd doping effect for a quasi-stoichiometric sample. The thin solid curve is for the non-stoichiometric Gd doping effect. Similarly, the dotted curve indicates the oxygen deficiency effect. These plots clearly show that Gd doping for both QS and non-stoichiometric EuO enhances the ferromagnetic interaction until 125 K and an oxygen deficiency further increases T_C to 160 K.

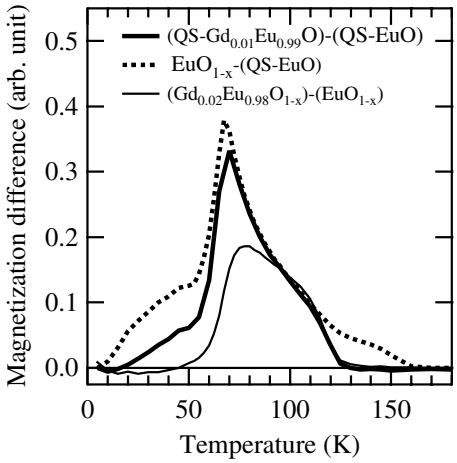

Figure 5. Differences in magnetization as a function of temperature.

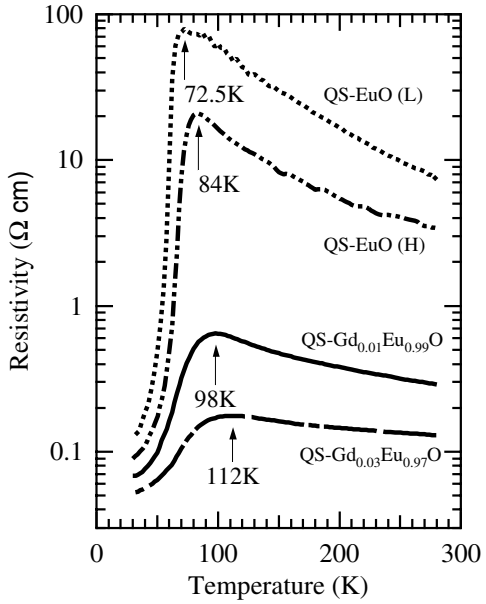

Figure 6. Temperature dependence of the resistivity. QS-EuO (L) and (H) were prepared with the same deposition rate and oxygen pressure. Arrows indicate maximum resistivity positions.

It is demonstrated that the enhanced magnetization via carrier electrons is dependent on the origin of the dopant.

5. Transport properties

The electrical resistivities of the QS-EuO, QS-$Gd_{0.01}Eu_{0.99}O$, and QS-$Gd_{0.03}Eu_{0.97}O$ were measured as a function of temperature. All samples in figure 6 exhibit a significant decrease in resistivity as the temperature decreases below ∼90 K. A similar drop in resistivity is reported

for EuO, $Gd_xEu_{1-x}O$ bulk, and EuO_{1-x} thin film [20–22]. Structural differences are not observed for Gd-doped and non-doped samples by XRD. Thus, the systematic decrease in the resistivity for Gd doping (figure 6) suggests that the primary origin of the resistivity behaviour of our samples is the change in carrier density. The arrows in the figure indicate the maximum resistivity R_{MAX} at the temperature T_{MAX}. The low vacancy film (QS-EuO (L)) shows $R_{MAX} = 79.5\ \Omega$ cm at 72.5 K, which is within the range of the reported single-crystal resistivity [20] and implies that the structural disorder in our film samples is comparable to single crystals. In a previous report for bulk samples, the temperature dependence of resistivity in the low temperature region ($<T_{MAX}$) is due to an increase in conduction electron density and a decrease in the magnetic scattering by ferromagnetic ordering as the temperature decreases [21]. The resistivity curve profiles of our films are similar to the bulk results and the temperature dependence is explained as follows. The resistivity increases as the temperature decreases in the same thermal exciting type as the semiconductor above T_{MAX}. The calculated activation energies of QS-EuO (L), QS-EuO (H), and QS-$Gd_xEu_{1-x}O$ ($x = 0.01$, 0.03) are 21.4, 11.75, 6.44, and 2.8 meV, respectively, as determined by Arrhenius plots. When the temperature decreases below T_C ($\sim$70 K), 4f spins at Eu^{2+} sites are aligned and the conduction band splits into spin up and down sub-bands. Since the magnetization increases as the temperature decreases, the conduction band splitting becomes larger. Finally, the lower energy sub-band falls below the donor level [21, 23]. Thus, the conduction electron density rapidly increases and there is an abrupt resistivity drop below T_C.

The actual film samples are not ideally stoichiometric. Consequently, there should be some oxygen vacancies that act like donors at least with the same concentration level as single-crystal EuO ($\sim 10^{18}$ cm^{-3} [8]). In figure 6, two quasi-stoichiometric films of EuO (L) and (H) show different resistivities. The same T_C was measured for both films as the bulk value ($T_C = 70$ K) and the temperature dependences of the magnetization agree with Brillouin's law, but T_C is not enhanced, which indicates that both vacancy concentrations N_L and N_H are less than N_C. Thus, EuO (L) and (H) are considered quasi-stoichiometric. A higher resistivity means a lower oxygen vacancy concentration. Therefore, the higher resistivity sample is named QS-EuO (L) and the lower one is QS-EuO (H). A small peak near T_{MAX} has been reported for some bulk EuO samples with low vacancy concentrations [20]. This anomaly was interpreted as a critical scattering effect by spin fluctuation [21, 24, 25]. Our films do not display this anomaly, which implies higher vacancy concentrations than that of ideal stoichiometric samples.

The difference between T_{MAX} and T_C for QS-EuO films is small and $T_C < T_{MAX}$. The T_Cs of QS-EuO (L) and (H) are the same, 70 K, and T_{MAX}s are 72.5 and 84.0 K, respectively. For QS-$Gd_xEu_{1-x}O$ ($x = 0.01$, 0.03) samples, T_Cs are the same, 125 K, and T_{MAX}s are 98.0 and 112.0 K. Unlike QS-EuO, $T_C > T_{MAX}$. The temperature dependence of the magnetization explains the differences in T_{MAX} for QS-EuO and QS-$Gd_xEu_{1-x}O$. For QS-$Gd_xEu_{1-x}O$, the magnetization gradually increases as the temperature decreases below T_C (125 K) and is significantly lower than $\sim$80 K as shown in figure 2. The long range ferromagnetic ordering is unstable in the range $\sim$80–125 K. Thus, the conduction band magnetic splitting below T_C (125 K) is small and the carrier electron gradually increases. The band splitting becomes significant as the magnetization increases at lower temperatures and the bottom of lower sub-band finally reaches the donor level. Then the doped electrons are introduced into the conduction band and the resistivity abruptly drops as plotted in figure 6. Therefore, T_{MAX} of Gd-doped films shifts to a higher temperature as the doping carrier concentration increases, but T_{MAX} is still lower than T_C. Although differences between EuO and $Gd_xEu_{1-x}O$ are qualitatively understood by the temperature dependence of the magnetization, the temperature dependence of carrier density, mobility, and the depth of impurity levels must be further investigated for a detailed understanding.

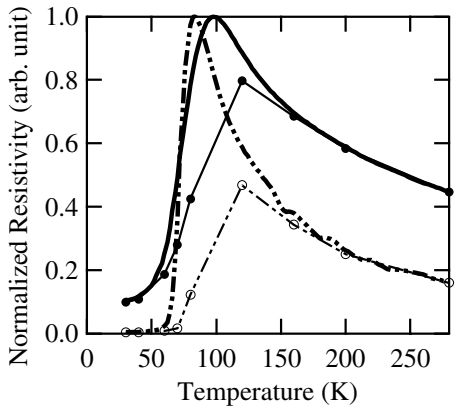

Figure 7. Relative resistivity as a function of temperature. The resistivity is normalized by maximum values. Both solid and dotted curves indicate QS-$Gd_{0.01}Eu_{0.99}O$ and QS-EuO results without external magnetic field. Solid and open circles are results of QS-$Gd_{0.01}Eu_{0.99}O$ and QS-EuO with a 1.5 T external field in sample plane.

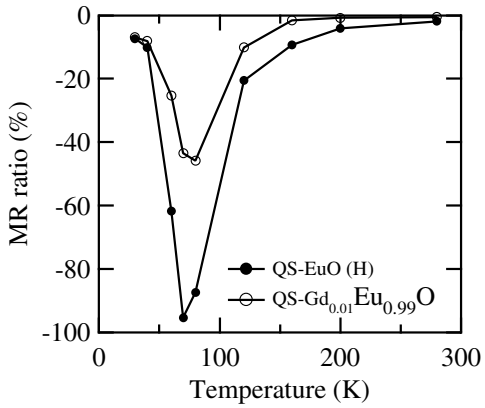

Figure 8. Magnetoresistance ratio as a function of temperature.

6. Magnetoresistance

Magnetoresistance measurements were performed using the same experimental set-up as the resistivity measurements with and without an external magnetic field. Figure 7 plots the normalized resistivity curves. The solid circles and open circles indicate the resistivities with 15 kOe applied magnetic field. Two plausible mechanisms explain the large magnetoresistance (MR) effect. The first is that the magnetization increases by applying magnetic field and the conduction band splits into up and down spin sub-bands due to the exchange interaction between the 4f and conduction electron spins. The bottom of the lower sub-band falls to the donor level and carrier electrons are introduced into the conduction sub-band. Thus, a large resistivity change appears when a magnetic field is applied. This mechanism is the same as the previous section and the effect of external magnetic field is equivalent to decreasing temperature. The other mechanism inhibits the Eu^{2+}-4f spin fluctuation by applying a field. The magnetic scattering decreases and the mobility of conduction electrons increases. Then a large MR effect is observed. If the first mechanism is dominant, the MR effect would follow

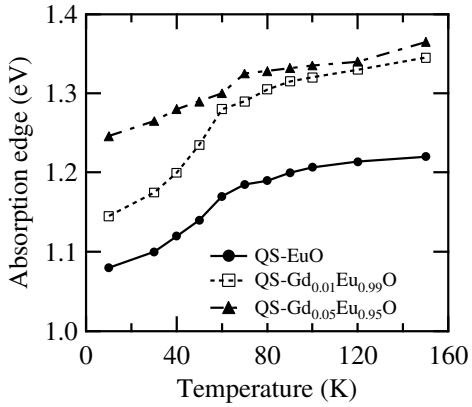

Figure 9. Temperature dependence of the absorption edge.

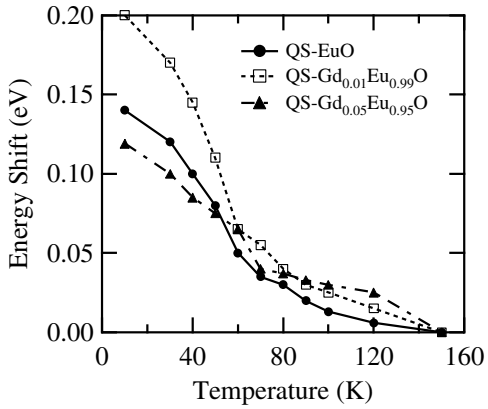

Figure 10. Relative energy shifts of absorption edge defined as $\Delta E_g = E_g\ (150\ \mathrm{K}) - E_g\ (T)$.

the magnetization behaviour. If the second mechanism is dominant, then the MR maximum should be near T_C due to a critical scattering phenomenon. Figure 8 plots the magnetoresistance ratio, which is defined as $\{R_{(H)} - R_{(0)}\}/R_{(0)}$. Both the MR ratio curves of QS-EuO and QS-$Gd_xEu_{1-x}O$ exhibit similar behaviour despite different T_C of 70 and 125 K. An anomaly due to the critical scattering phenomenon is not observed around T_C (125 K) of the QS-$Gd_xEu_{1-x}O$ film. Both these results indicate that the magnetic scattering mechanism is not dominant. The maximum changes of MR ratio (minimum peak) for both samples appear between 70 and 80 K. The magnetization curves of both samples exhibit the largest change at the temperature as illustrated in figure 2. Consequently, the increasing carrier density on conduction sub-band splitting plays the primary role in the MR effect for our films.

7. Energy shift of the fundamental absorption edge

The absorption spectra are measured between 1.0 and 1.7 eV photon energy using a conventional optical spectrometer system. The absorption edge E_g is determined by extrapolating the absorption curve to zero and figure 9 displays the temperature dependences. All the samples show a red shift in E_g as the temperature decreases. If this absorption is

attributed to the electron transition from the 4f state to the 5d conduction band, then the red shift is explained by conduction band splitting [26, 27]. The up and down spin conduction band splitting increases as the magnetic interaction increases on lowering temperature and the energy gap between the bottom of the lower conduction sub-band and the 4f state decreases. Figure 10 plots the energy shifts, which are defined as $\Delta E_g = E_g(150\ \mathrm{K}) - E_g(T)$ and are calculated from figure 9, to clearly display the bandgap behaviours. The energy shifts at 10 K are 0.14, 0.20, and 0.12 eV for QS-EuO, QS-$Gd_{0.01}Eu_{0.99}O$, and QS-$Gd_{0.05}Eu_{0.95}O$, respectively. Schoenes *et al* reported a similar result and proposed that the shift energy directly represents the exchange energy [26]. The energy of the conduction electron $E_{(k)}$ is written as

$$E_{(k)} = E^0_{(k)} \pm \frac{JS\sigma}{2}, \tag{1}$$

where $E^0_{(k)}$, J, S, and σ are the energy of the degenerate conduction band, the exchange interaction, the spin of Eu^{2+}, and the polarization of conduction electrons, respectively [8]. For a splitting conduction band, σ is unity. Since $JS/2$ corresponds to ΔE_g, the estimated J values are 80, 110, and 69 meV at 10 K for QS-EuO, QS-$Gd_{0.01}Eu_{0.99}O$, and QS-$Gd_{0.05}Eu_{0.95}O$, respectively. Thus, the exchange energy of QS-$Gd_{0.05}Eu_{0.95}O$ is only 60% of QS-$Gd_{0.01}Eu_{0.99}O$ and the $Gd_xEu_{1-x}O$ ($x < 0.02$) is 50% of EuO for Schoenes's single-crystal result, which implies that the exchange interactions J_1 and J_2 of some Gd-doped samples disappear below 40 K by the Heisenberg model. However, this significant anomaly is not observed in our magnetization measurements below 70 K. A more thorough explanation is necessary to understand the energy shift.

A large sample dependence of the absorption edge in figure 9 indicates a blue shift with Gd doping, which contradicts previous reports [26]. The most probable explanation for the blue shift is a lattice distortion. However, meaningful changes in lattice constant are not observed in our XRD measurements [18]. Thus, the reason is not a simple lattice distortion, but a complex structural change. The blue shift mechanism and the difference between thin films and bulk samples are not well understood.

Conduction band splitting also explains the energy shifts between 80 and 150 K in figure 10. All three energy shift curves gradually increase as the temperature decreases from 150 K and is significant below 70 K. Since the Eu^{2+}–Eu^{2+} indirect exchange interactions J_1 and J_2 disappear above 70 K, the energy shift at 80–150 K represents the magnetic splitting of the conduction band derived from d–f exchange interaction via conduction electrons. The remaining finite energy shift of QS-EuO above T_C (70 K) suggests a magnetic interaction in this temperature range. Short range ordering via doped electrons and a small oxygen deficiency may occur. Both Gd doped samples show larger energy shifts than QS-EuO above 80 K (figure 10), which implies that the d–f exchange interactions are strong enough to enhance T_C. These observations are consistent with the magnetization results in figures 2 and 4.

8. Conclusion

Two different n-type doped EuO films, Gd-doped EuO and oxygen deficient EuO_{1-x} (non-stoichiometric EuO), were prepared using a reactive deposition method in a MBE system. Gadolinium-doped films exhibited similar magnetic and electrical transport properties as bulk samples. The physical properties are sensitive to the Gd doping level and the oxygen stoichiometry, which implies that carrier electron density is a primary factor for the physical properties. Both n-type doped samples show different enhancements in T_C. The basic enhancement mechanism is explained by the increase in the indirect exchange interaction via carrier electrons. Gadolinium doping increases T_C up to 125 K. On the other hand, the oxygen

non-stoichiometry enhances T_C above 150 K. Each electron doping creates different donor levels. Hence, different temperature dependences of the electron transfer to the conduction band are observed. The resistivities as a function of temperature for QS-EuO and QS-$Gd_xEu_{1-x}O$ have a maximum R_{MAX} at T_{MAX} and significantly decrease below T_{MAX} due to the increased carrier density. The primary part of the resistivity behaviour and the large MR effect are explained by a simple conduction band magnetic splitting mechanism. The absorption edge results are dependent on the sample, but are reasonably explainable by the band splitting mechanism. On the other hand, the unusual blue shift observed for Gd doping samples is derived from non-magnetic factors, which require further investigation.

Acknowledgment

This work was supported by a Grant-in-Aid for Scientific Research from the Ministry of Education, Science and Culture of Japan.

References

[1] Wolf S A, Awschalom D D, Buhrman R A, Daughton J M, von Molnár S, Roukes M L, Chtchelkanova A Y and Treger D M 2001 *Science* **294** 1488
[2] Koshihara S, Oiwa A, Hirasawa M, Katsumoto S, Iye Y, Urano C, Takagi H and Munekata H 1997 *Phys. Rev. Lett.* **78** 4617
[3] Ohno H 1998 *Science* **281** 951
[4] Dietl T and Ohno H 2001 *Physica* E **9** 185
[5] Ohno H, Chiba D, Matsukura F, Omiya T, Abe E, Dietl T, Ohno Y and Ohtani K 2000 *Nature* **408** 944
[6] Yamada K and Kamata N 1992 *J. Magn. Magn. Mater.* **104–107** 991
[7] Moodera J S, Hao X, Gibson G A and Meservay R 1988 *Phys. Rev. Lett.* **61** 637
[8] Mauger A and Godart C 1986 *Phys. Rep.* **141** 51
[9] Kawaguchi K and Sohma M 1994 *Thin Solid Films* **246** 1
[10] Kawaguchi K, Sohma M and Oosawa Y 1995 *J. Magn. Magn. Mater.* **148** 80
[11] Iwata N, Pindoria G, Morishita T and Kohn K 2000 *J. Phys. Soc. Japan* **69** 230
[12] Iwata N, Morishita T and Kohn K 2000 *J. Phys. Soc. Japan* **69** 1745
[13] Konno T J, Ogawa N, Wakoh K, Sumiyama K and Suzuki K 1996 *Japan. J. Appl. Phys.* **35** 6052
[14] Konno T J, Wakoh K, Sumiyama K and Suzuki K 1998 *Japan. J. Appl. Phys.* **37** L787
[15] Mauger A, Escorne M, Godart C, Desfours J P and Achard J C 1980 *J. Physique Coll.* **41** C5 265
[16] Borukhovich A S, Bamburov V G and Sidorov A A 1988 *J. Magn. Magn. Mater.* **73** 106
[17] Mauger A 1977 *Phys. Status Solidi* b **84** 761
[18] Matsumoto T, Yamaguchi K, Yuri M, Kawaguchi K, Koshizaki N and Yamada K 2004 *Trans. Magn. Soc. Japan* at press
[19] Suzuki M, Matsumoto T, Yamaguchi K, Kawaguchi K, Koshizaki N and Yamada K 2004 to be submitted
[20] Oliver M R, Dimmock J O, McWhorter A L and Reed T B 1972 *Phys. Rev.* B **5** 1078
[21] Von Molnar S and Shafer M W 1970 *J. Appl. Phys.* **41** 1093
[22] Massenet O, Capiomont Y and Van Dang N 1974 *J. Appl. Phys.* **45** 3593
[23] Oliver M R, Kafalas J A, Dimmock J O and Reed T B 1970 *Phys. Rev. Lett.* **24** 1064
[24] de Gennes P G and Friedel T 1958 *J. Phys. Chem. Solids* **4** 71
[25] Von Molnar S and Kasuya T 1968 *Phys. Rev. Lett.* **21** 1757
[26] Schoenes J and Wachter P 1974 *Phys. Rev.* B **9** 3097
[27] Schiller R and Nolting W 2001 *Solid State Commun.* **118** 173